Monthly Notices
of the
ROYAL ASTRONOMICAL SOCIETY

MNRAS **448,** 2617–2623 (2015) doi:10.1093/mnras/stv197

High-precision multiband time series photometry of exoplanets Qatar-1b and TrES-5b

D. Mislis,[1⋆] L. Mancini,[2] J. Tregloan-Reed,[3] S. Ciceri,[2] J. Southworth,[4] G. D'Ago,[5] I. Bruni,[6] Ö. Baştürk,[7] K. A. Alsubai,[1] E. Bachelet,[1] D. M. Bramich,[1] Th. Henning,[2] T. C. Hinse,[8] A. L. Iannella,[5] N. Parley[1] and T. Schroeder[2]

[1]*Qatar Environment and Energy Research Institute, Qatar Foundation, Tornado Tower, Floor 19, PO Box 5825, Doha, Qatar*
[2]*Max Planck Institute for Astronomy, Königstuhl 17, D-69117 Heidelberg, Germany*
[3]*NASA Ames Research Center, Moffett Field, CA 94035, USA*
[4]*Astrophysics Group, Keele University, Staffordshire ST5 5BG, UK*
[5]*Department of Physics, University of Salerno, Via Giovanni Paolo II, I-84084 Fisciano (SA), Italy*
[6]*INAF – Osservatorio Astronomico di Bologna, Via Ranzani 1, I-40127 Bologna, Italy*
[7]*Department of Astronomy and Space Sciences, Faculty of Science, Ankara University, Tandoğan, TR-06100 Ankara, Turkey*
[8]*Korea Astronomy and Space Science Institute, 776 Daedukdae-ro, Yuseong-gu, Daejeon 305-348, Republic of Korea*

Accepted 2015 January 27. Received 2015 January 27; in original form 2014 October 21

ABSTRACT

We present an analysis of the Qatar-1 and TrES-5 transiting exoplanetary systems, which contain Jupiter-like planets on short-period orbits around K-dwarf stars. Our data comprise a total of 20 transit light curves obtained using five medium-class telescopes, operated using the defocusing technique. The average precision we reach in all our data is $\mathrm{RMS_Q} = 1.1$ mmag for Qatar-1 ($V = 12.8$) and $\mathrm{RMS_T} = 1.0$ mmag for TrES-5 ($V = 13.7$). We use these data to refine the orbital ephemeris, photometric parameters, and measured physical properties of the two systems. One transit event for each object was observed simultaneously in three passbands (*gri*) using the BUSCA imager. The QES survey light curve of Qatar-1 has a clear sinusoidal variation on a period of $P_\star = 23.697 \pm 0.123$ d, implying significant star-spot activity. We searched for star-spot crossing events in our light curves, but did not find clear evidence in any of the new data sets. The planet in the Qatar-1 system did not transit the active latitudes on the surfaces of its host star. Under the assumption that $P_\star$ corresponds to the rotation period of Qatar-1A, the rotational velocity of this star is very close to the $v \sin i_\star$ value found from observations of the Rossiter–McLaughlin effect. The low projected orbital obliquity found in this system thus implies a low absolute orbital obliquity, which is also a necessary condition for the transit chord of the planet to avoid active latitudes on the stellar surface.

Key words: techniques: photometric – planets and satellites: detection – planets and satellites: fundamental parameters – planetary systems.

1 INTRODUCTION

Ground-based photometric surveys have found a large number of transiting planets, possessing a huge diversity in their physical and orbital properties. The precise characterization of these objects is a challenge as it requires high-quality data, both photometric and spectroscopic. The main limitation to our understanding of most transiting planets is due to the quality of the transit light curve, which is critical in determining the properties of both the planets and their host stars (Southworth 2008, 2009).

In this work, we present follow-up photometry of two transiting planets orbiting cool stars – Qatar-1b and TrES-5b – aimed at not only improving measurements of their physical properties but also investigating the spot activity of their host stars. Our new data allow a significant improvement in our understanding of both systems and, in the case of TrES-5, form the basis of the first study of the system since the discovery paper.

Qatar-1b was discovered by Alsubai et al. (2011), and was the first planet found by the Qatar Exoplanet Survey (QES), an exoplanet transit survey focused on hot Jupiters and hot Neptunes via the transit method (Alsubai et al. 2013). The transiting planet TrES-5b was discovered shortly afterwards (Mandushev et al. 2011) using observations by the TrES survey (Alonso et al. 2004). The Qatar-1

⋆ E-mail: dmislis@qf.org.qa

Table 1. Summary of observations of Qatar-1 and TrES-5.

Telescope	Date	Start (UT)	End (UT)	Frames (No)	Exp (s)	Filter	Airmass	Moon (per cent)	Apertures (pixel)	RMS (10^{-4})
Qatar-1:										
CAHA 1.23 m	2011.08.25	23:55	03:36	158	60	Cousins *R*	1.20→1.76	12.8	9,25,35	12.6
CAHA 2.2 m	2011.08.25	23:46	04:39	115	60	Gunn *g*	1.19→2.20	12.8	16.5,64.9,78.3	10.5
CAHA 2.2 m	2011.08.25	23:46	04:39	117	60	Gunn *r*	1.19→2.20	12.8	17,36.1,70	7.4
CAHA 2.2 m	2011.08.25	23:46	04:39	118	60	Gunn *i*	1.19→2.20	12.8	13.2,38.9,61.9	9.6
CAHA 1.23 m	2012.07.21	20:32	00:34	112	120	Cousins *R*	1.33→1.13	8.0	7.9,31.9,45	7.1
CAHA 1.23 m	2012.09.11	00:27	03:48	78	120	Cousins *R*	1.36→2.20	27.1	19.9,38.9,53	7.5
CAHA 1.23 m	2013.06.14	20:48	00:30	95	120	Cousins *R*	1.73→1.19	19.3	12.2,41,50.2	8.8
CAHA 1.23 m	2013.07.28	20:17	01:05	156	120	Cousins *R*	1.31→1.16	59.1	25.8,39,61	7.3
CAHA 1.23 m	2014.04.19	01:40	04:38	109	160	Cousins *R*	1.61→1.17	80.1	19,29,50	25.6
CAHA 1.23 m	2014.06.04	20:42	02:57	138	150	Cousins *R*	1.97→1.13	12.9	20,30,50	7.7
TUG100	2014.06.04	21:39	01:42	98	120	Cousins *R*	1.69→1.16	12.9	20,30,35	14.0
CAHA 1.23 m	2014.09.07	23:57	04:37	135	96–135	Cousins *R*	1.25→2.32	98.2	22,40,60	11.8
TrES-5:										
CAHA 2.2 m	2011.08.26	20:55	00:55	95	60	Gunn-*g*	1.02→1.57	7.0	10.2,45.4,56.5	12.3
CAHA 2.2 m	2011.08.26	20:55	00:55	88	60	Gunn-*r*	1.02→1.57	7.0	17.3,42.1, 55.6	8.5
CAHA 2.2 m	2011.08.26	20:55	00:55	91	60	Gunn-*i*	1.02→1.57	7.0	10,28,39.1	12.1
CAHA 1.23 m	2012.09.10	19:21	23:36	77	170	Cousins *R*	1.11→1.21	29.0	16,40.1,54.8	8.5
CAHA 1.23 m	2013.06.15	00:42	03:50	65	125	Cousins *R*	1.14→1.11	44.9	12,38,55.3	9.0
CAHA 1.23 m	2013.07.30	23:10	04:03	128	120	Cousins *I*	1.08→1.47	38.2	13.7,27.8,46	11.3
Cassini 1.52 m	2013.09.14	21:19	02:59	139	180	Gunn *r*	1.08→2.09	78.2	9.8,22.6,38.7	13.0
INT 2.5 m	2013.09.14	21:04	22:22	37	120	Cousins *I*	1.05→1.17	72.4	18,28,50	4.1

and TrES-5 systems are notably similar in terms of orbital period (1.4–1.5 d), host star effective temperature (4800–5200 K) and metallicity ($\left[\frac{\mathrm{Fe}}{\mathrm{H}}\right] = 0.20$), and the planetary radius ($\sim$1.2 R_{Jup}) and equilibrium temperature (1400–1500 K). Qatar-1 has subsequently been studied by Covino et al. (2013), who found a sky-projected orbital obliquity consistent with axial alignment, and by von Essen et al. (2013), who found indications of transit timing variations (TTVs) in this system. No studies of TrES-5 have been published since its discovery paper (Mandushev et al. 2011).

The possibility to observe occulted star-spots during planetary-transit events opens new opportunities in the understanding of stars in general and planetary systems in particular. Those spots which are occulted by the planet manifest themselves as a small increase in flux during transit, which can be modelled to obtain the spot size, position, and temperature (e.g. Mancini et al. 2014). Multiple observations of the same spot during different transits can yield the orbital obliquity of the system (Nutzman, Fabrycky & Fortney 2011; Sanchis-Ojeda et al. 2011) to a significantly higher precision than achievable via the Rossiter–McLaughlin effect (Tregloan-Reed, Southworth & Tappert 2013). The wavelength dependence of the amplitude of the unocculted star-spots can mimic changes in the apparent radius of transiting planets as a function of wavelength (Pont et al. 2013; Oshagh et al. 2014).

In this work, we present high-precision photometric observations of Qatar-1 and TrES-5, and use them to get more accurate measurements of the physical parameters of the systems. Some of our data were obtained in multiple passbands simultaneously, but we find no evidence for spot crossings in these data. We do, however, find strong evidence that the Qatar-1A is a spotted star from the long-term light curve of the system.

2 OBSERVATIONS AND DATA REDUCTION

Our observations were obtained using five medium-size telescopes equipped with imaging instruments, and operated out of focus (see Southworth et al. 2009). A summary of the observations is given in Table 1. The data were reduced using the DEFOT pipeline from Southworth et al. (2009, 2014). This pipeline was used to debias and flat-field the data, then perform aperture photometry on the target and all possible comparison stars. The radii of the software apertures (target, inner sky, outer sky) for each data set were chosen to give the lowest scatter in the final light curve. The final light curve was constructed by calculating differential magnitudes versus a weighted set of comparison stars. The weights were optimized simultaneously with the coefficients of a low-order polynomial of magnitude versus time, in order to rectify the light curve to zero differential magnitude and minimize the scatter of the data obtained outside transit.

The data were reduced using the method and the DEFOT pipeline from Southworth et al. (2009, 2014).

A total of 11 transits were observed using the 1.23 m telescope at Centro Astronómico Hispano-Alemán (CAHA). This uses a 2048 × 2048 pixel CCD camera with a plate scale of 0.32 arcsec pixel^{-1} and has a 21.5 arcmin × 21.5 arcmin field of view with the default *BVRI* filters. 10 of the transits were obtained through a Cousins *R* filter and the last through a Cousins *I* filter. The first three transits were already presented in the study by Covino et al. (2013) but were re-reduced for the current work.

One transit each of Qatar-1 and TrES-5 was observed using the CAHA 2.2 m telescope equipped with the BUSCA instrument. This obtains CCD images of a 5.8 arcmin diameter field of view simultaneously in four optical passbands, split by dichroic elements. Each of the four CCDs has 4096 × 4096 pixels and is operated using 2 × 2 binning. For both transits we obtained useful data in the Thuan–Gunn *g*, *r*, and *i* passbands. The data taken through the Strömgren *u* filter were discarded due to high scatter: both objects are comparatively faint ($V = 12.8$ for Qatar-1 and $V = 13.7$ for TrES-5) and cool so have very low flux levels in this passband.

One transit of Qatar-1 was monitored with the 1.0 m telescope (T100) at TÜBİTAK National Observatory (TUG) in Turkey,

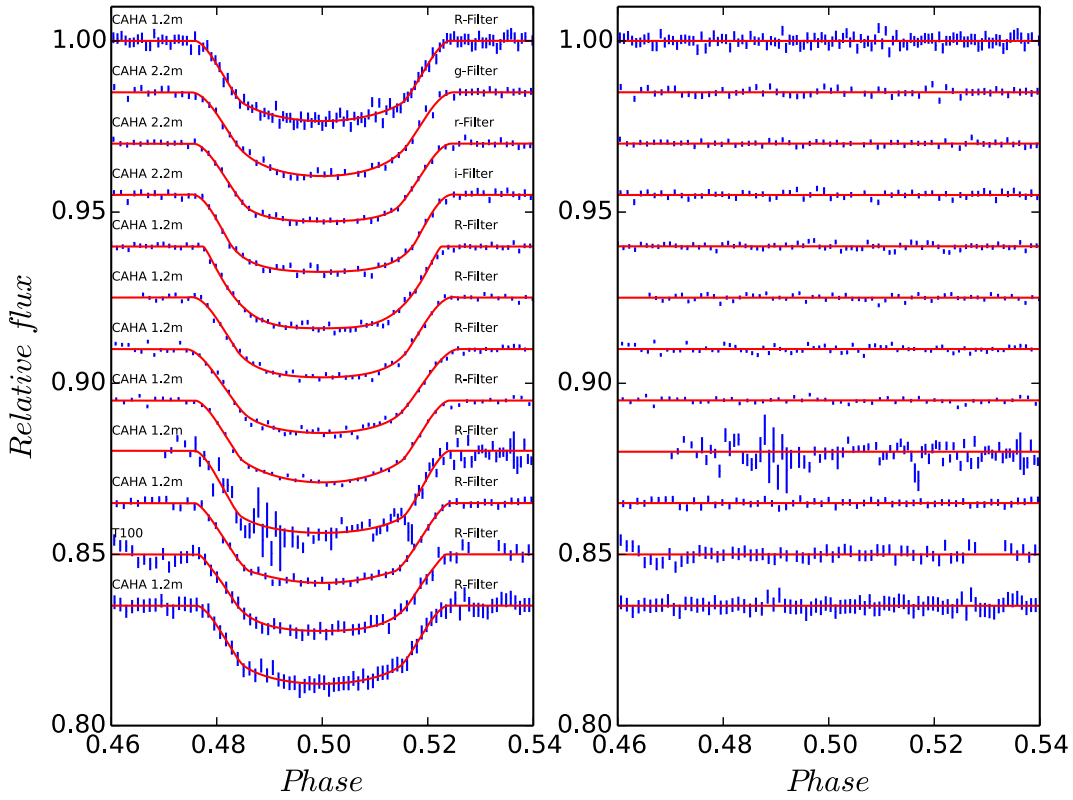

Figure 1. Left: our light curves of Qatar-1 (blue points) with the JKTEBOP best fits (red lines) overplotted. The telescope and filter used for each data set are labelled. Right: the residuals of each fit.

equipped with a 4096 × 4096 pixel CCD with a field of view of 21.5 arcmin × 21.5 arcmin. The transit was observed through a Cousins *R* filter.

One transit of TrES-5 was obtained using the 2.5 m Isaac Newton Telescope (INT) at La Palma, Spain, and the Wide Field Camera (WFC). This is a mosaic of four CCDs of which we used only CCD4, to avoid possible systematic errors and calibration issues resulting from the use of multiple CCDs in the mosaic. This CCD has 2048 × 4096 pixels, giving a field of view of 11.3 arcmin × 22.5 arcmin, and a Cousins *I* filter was selected.

Finally, a transit of TrES-5 was observed using the Cassini 1.52 m telescope at Bologna Astronomical Observatory, Loiano, Italy. The BFOSC instrument was used in imaging mode, with a Thuan–Gunn *r* filter. The 1024 × 1024 pixel CCD provided a field of view of 13 arcmin × 12.6 arcmin at 0.58 arcsec pixel^{-1}.

3 TRANSIT ANALYSIS

Each transit light curve was modelled with the JKTEBOP code to extract measurements of its photometric parameters. The object size parameters in JKTEBOP are the fractional radii of the star and the planet (r_A and r_b), which are the ratios between the true radii and the semimajor axis ($r_{A,b} = \frac{R_{A,b}}{a}$). The fitted parameters were the sum of the fractional radii ($r_A + r_b$), the ratio of the radii ($k = \frac{r_b}{r_A} = \frac{R_b}{R_A}$), the orbital inclination (i), and a reference time of mid-transit. We assumed an orbital eccentricity of zero for both objects based on previous studies (Mandushev et al. 2011; Covino et al. 2013). Limb darkening was applied using the quadratic law, with coefficients taken from Claret (2004b). We used Monte Carlo simulations to perform the error analysis for each transit fit. The errors were propagated following Alonso et al. (2008) and Mislis et al. (2010).

3.1 Qatar-1

For Qatar-1, we collected 12 light curves in total (see Fig. 1). We fit each of the data sets individually, obtaining the parameter values given in Table 2. The parameter values in Table 2 were combined into weighted means for the determination of the physical properties of the system (see below). We then fitted the T_0 values with a straight line versus cycle number to determine the orbital ephemeris. The uncertainties were obtained using 1000 Monte Carlo simulations. The resulting ephemeris is

$$T_0 = 2455\,799.579\,54(4) + 1.420\,025\,86(275) \cdot E, \quad (1)$$

where T_0 is the transit mid-time, E is the cycle number and the bracketed quantities give the uncertainty in the final digit of the preceding number. All times in our analysis were converted to Barycentric Julian Day (BJD/TDB).

We supplemented our T_0 values with data from the literature and searched for TTVs. We included timings from the ETD amateur data base[1] with quality higher than 3. We fit a linear function to T_0 and then removed the linear trend. Fig. 2 shows the results (O − C diagram) overplotted with the best linear fit. The χ^2_{red} value is 31.4, which is very high. This implies that the O − C data cannot be explained by a simple linear fit, but still the amplitude of our O − C residuals are smaller ($RMS_{O-C} = 1.50$ min) than von Essen et al. (2013) ($RMS_{O-C} = 1.67$ min), Covino et al. (2013)

[1] http://var2.astro.cz/ETD/

Table 2. Fitted parameter values for each light curve of Qatar-1.

Date	$r_A + r_b$	k	r_A	r_b	Inclination (°)	T_0 (BJD/TDB)
2011.08.25	0.178 ± 0.011	0.1455 ± 0.0039	0.155 ± 0.009	0.0226 ± 0.0018	84.64 ± 0.84	55799.5759 ± 0.0002
2011.08.25	0.179 ± 0.009	0.1469 ± 0.0039	0.156 ± 0.007	0.0229 ± 0.0016	84.62 ± 0.66	55799.5755 ± 0.0001
2011.08.25	0.184 ± 0.009	0.1467 ± 0.0041	0.160 ± 0.007	0.0235 ± 0.0016	84.02 ± 0.73	55799.5758 ± 0.0002
2011.08.25	0.172 ± 0.011	0.1428 ± 0.0031	0.150 ± 0.009	0.0215 ± 0.0018	85.18 ± 0.89	55799.5756 ± 0.0001
2012.07.21	0.185 ± 0.004	0.1500 ± 0.0022	0.161 ± 0.004	0.0241 ± 0.0008	83.95 ± 0.32	56130.4430 ± 0.0001
2012.09.11	0.178 ± 0.007	0.1461 ± 0.0028	0.155 ± 0.006	0.0226 ± 0.0010	84.50 ± 0.52	56181.5668 ± 0.0001
2013.06.14	0.197 ± 0.006	0.1524 ± 0.0024	0.171 ± 0.004	0.0260 ± 0.0010	83.33 ± 0.34	56458.4665 ± 0.0002
2013.07.28	0.183 ± 0.006	0.1480 ± 0.0020	0.159 ± 0.004	0.0235 ± 0.0010	84.10 ± 0.42	56502.4905 ± 0.0002
2014.04.19	0.176 ± 0.018	0.1471 ± 0.0083	0.153 ± 0.015	0.0226 ± 0.0030	84.91 ± 1.50	56766.6120 ± 0.0004
2014.06.04	0.181 ± 0.009	0.1458 ± 0.0028	0.158 ± 0.007	0.0231 ± 0.0014	84.41 ± 0.66	56813.4731 ± 0.0002
2014.06.04	0.182 ± 0.020	0.1446 ± 0.0076	0.159 ± 0.016	0.0230 ± 0.0032	84.10 ± 1.50	56813.4720 ± 0.0003
2014.09.07	0.173 ± 0.011	0.1427 ± 0.0035	0.151 ± 0.009	0.0216 ± 0.0018	83.86 ± 0.80	56908.6149 ± 0.0002
Weighted mean	0.184 ± 0.002	0.1475 ± 0.0009	0.160 ± 0.002	0.0236 ± 0.0004	84.03 ± 0.16	

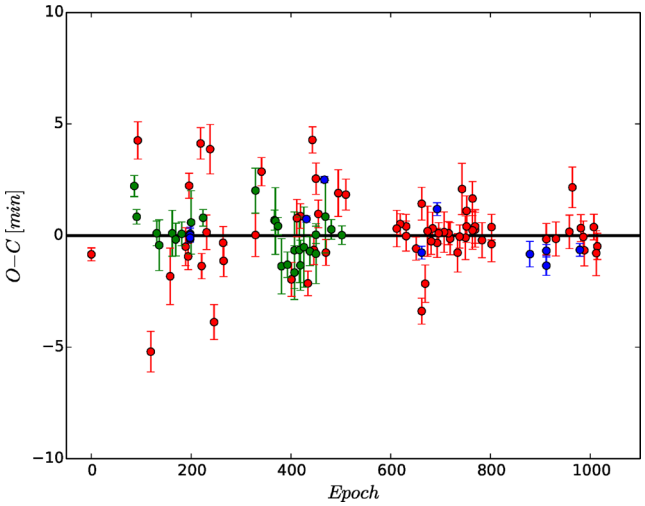

Figure 2. O − C diagram for the transit times of Qatar-1. Our own data are shown using blue dots, 26 data points from von Essen et al. (2013, green dots), and the 69 additional light curves from ETD data base (red dots).

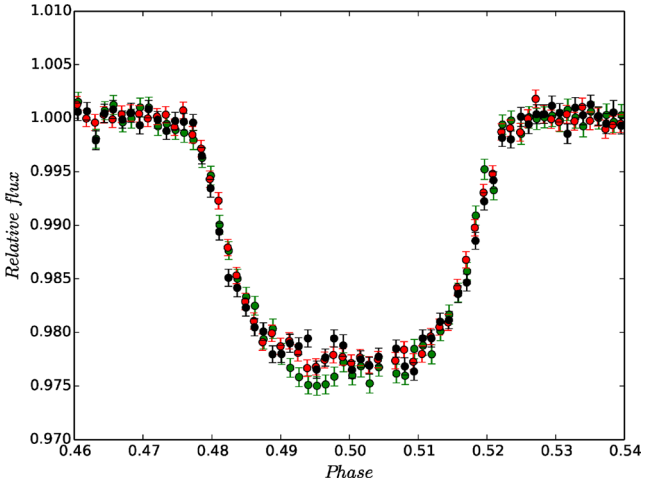

Figure 3. The BUSCA light curves of Qatar-1. Green, red and black points show the *g*, *r*, and *i* data, respectively.

(RMS$_{O-C}$ = 2.45 min), or ETD (RMS$_{O-C}$ = 3.85 min). von Essen et al. (2013) found evidence for TTVs in Qatar-1 but we need further and more precise data in order to analyse this scenario in detail.

3.2 Multiband photometry of Qatar-1

The BUSCA light curves were obtained simultaneously in three filters using the same telescope and instrument, so are useful for investigating the possible presence of star-spots. Fig. 3 shows the three light curves overplotted. Whilst there are suggestions of star-spots in the *g* and *r* data, these are close to the level of the noise so their existence is not proven. This transit was also monitored using the CAHA 1.23 m telescope (first data set in Fig. 1), and these data do not confirm the presence of any star-spots.

Whilst we have no clear detection of star-spots via occultation during transit, spots are a common phenomenon on the surfaces of K-type dwarfs. They can cause brightness modulation at the rotational period (and/or its submultiples) of the star. We used the discovery light curves from QES (Alsubai et al. 2011), which span 380 d, to search for stellar variability. A Lomb–Scargle periodogram of the data shows a clear detection of sinusoidal modulation at a period of $P_\star$ = 23.697 ± 0.123 d (Fig. 4), which

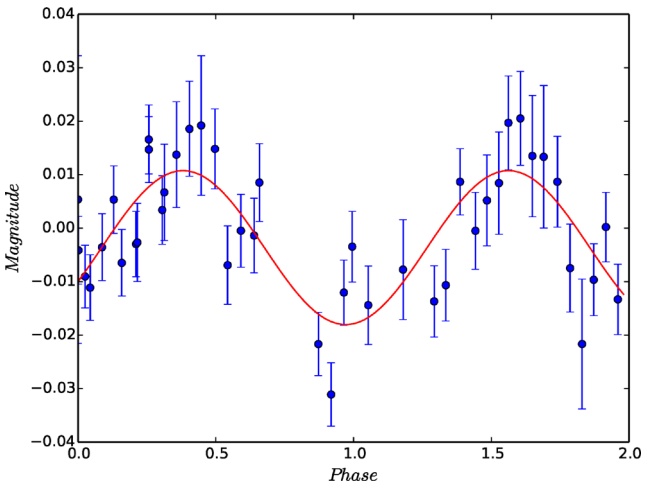

Figure 4. Long-term light curve of Qatar-1 from QES, phase-folded on a period of 23.697 d. The best fit is shown by a red line.

Table 3. Fitted parameter values for each light curve of TrES-5.

Date	$r_A + r_b$	k	r_A	r_b	Inclination (°)	T_0 (BJD/TDB)
2011.08.26	0.180 ± 0.016	0.144 ± 0.007	0.157 ± 0.013	0.0227 ± 0.0028	85.04 ± 1.42	55800.4753 ± 0.0002
2011.08.26	0.198 ± 0.006	0.146 ± 0.002	0.172 ± 0.005	0.0252 ± 0.0011	83.58 ± 0.42	55800.4744 ± 0.0002
2011.08.26	0.194 ± 0.014	0.135 ± 0.005	0.171 ± 0.011	0.0232 ± 0.0022	83.79 ± 0.90	55800.4751 ± 0.0003
2012.09.10	0.184 ± 0.014	0.139 ± 0.005	0.161 ± 0.011	0.0225 ± 0.0022	84.87 ± 0.98	56181.4120 ± 0.0002
2013.06.15	0.188 ± 0.008	0.145 ± 0.002	0.164 ± 0.007	0.0238 ± 0.0015	84.55 ± 0.58	56458.5923 ± 0.0001
2013.07.30	0.170 ± 0.010	0.141 ± 0.005	0.149 ± 0.008	0.0210 ± 0.0015	85.10 ± 0.84	56504.5419 ± 0.0001
2013.09.14	0.184 ± 0.014	0.145 ± 0.005	0.161 ± 0.011	0.0232 ± 0.0002	85.48 ± 0.91	56550.4919 ± 0.0001
2013.09.14	0.180 ± 0.014	0.139 ± 0.005	0.158 ± 0.011	0.0220 ± 0.0022	84.26 ± 1.03	56550.4915 ± 0.0001
Weighted mean	0.188 ± 0.004	0.143 ± 0.0012	0.164 ± 0.003	0.0232 ± 0.0002	84.27 ± 0.26	

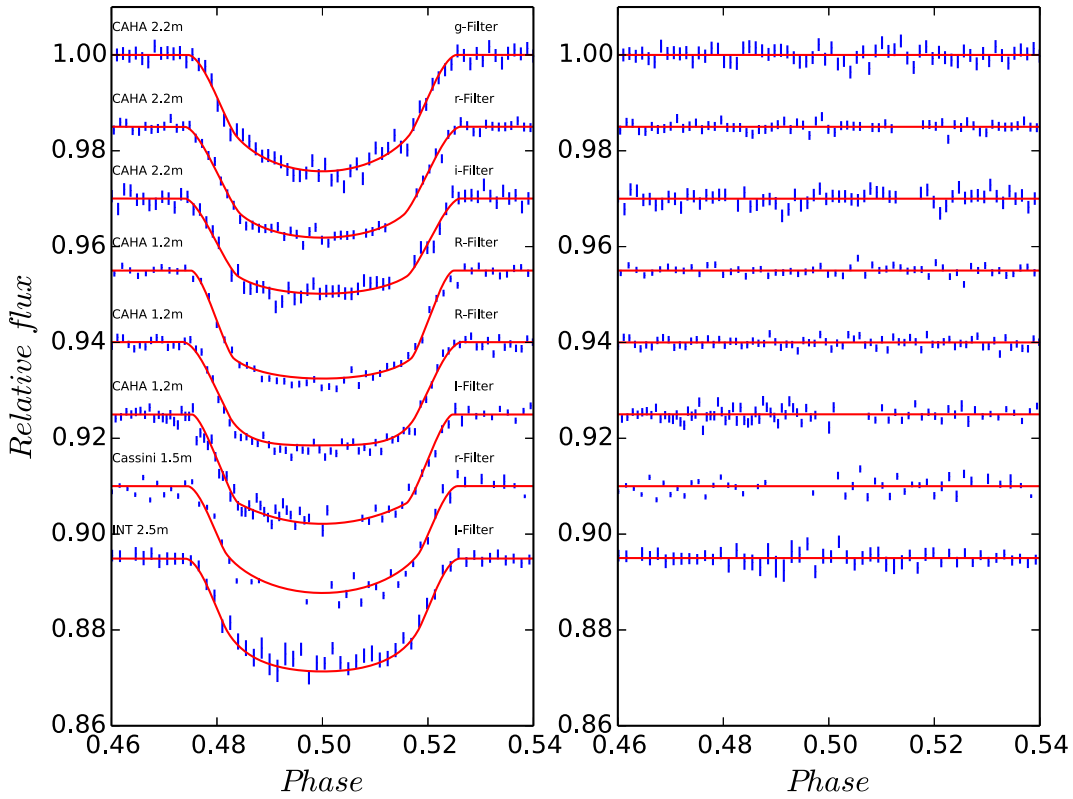

Figure 5. Left: our light curves of TrES-5 (blue points) with the JKTEBOP best fits (red lines) overplotted. The telescope and filter used for each data set are labelled. Right: the residuals of each fit.

we take to be the rotational period of the star. The implied stellar rotation velocity of $v = 1.76\,\mathrm{km\,s^{-1}}$ is fully consistent with the value of $v \sin i_\star = 1.7 \pm 0.3\,\mathrm{km\,s^{-1}}$ found by Covino et al. (2013) from the Rossiter–McLaughlin effect. This in turn indicates that the inclination of the stellar rotation axis, $i_\star$, is close to 90°, so the *true* orbital obliquity of the system is close to the measured value of the *projected* orbital obliquity found by Covino et al. (2013).

3.3 TrES-5b

The analysis of our eight light curves of TrES-5 followed the same steps as for Qatar-1 above. The best-fitting photometric parameters are given in Table 3 and the best fits are plotted in Fig. 5. The parameter values in Table 3 were combined into weighted means for the determination of the physical properties of the system (see below). The resulting orbital ephemeris is

$$T_0 = 2456\,458.592\,19(9) + 1.482\,246\,86(614) \cdot E. \quad (2)$$

As with Qatar-1, we added T_0 measurements from the ETD data base (again using only those with qualities higher than 3) and formed the O − C diagram (Fig. 6). The best-fitting ephemeris has $\chi^2_{\rm red} = 7.15$, which a factor of 10 lower than that for Qatar-1. This $\chi^2_{\rm red}$ indicates either that the linear ephemeris is a poor representation of the data or that the error bars of many of the T_0 values are underestimated. As with Qatar-1, further data are needed to investigate this situation and to provide clear evidence (or otherwise) of the presence of TTVs in this system.

The multiband data from BUSCA are shown in Fig. 7, and contain no clear evidence of star-spot occultations. The data during totality (between second and third contact) are rather noisy so are not good

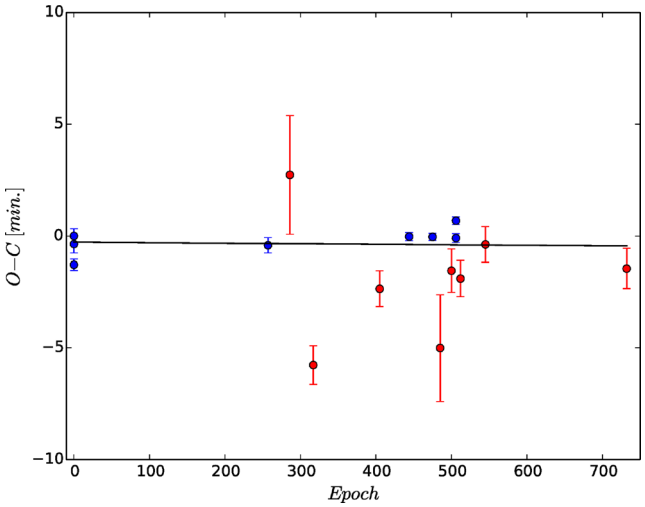

Figure 6. O − C diagram for the transit times of TrES-5. Our own data are shown using blue dots and the eight additional light curves from ETD data base are shown with red dots.

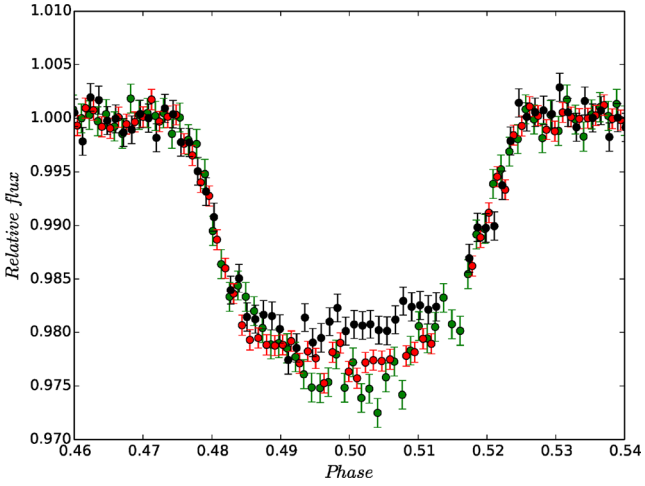

Figure 7. The BUSCA light curves of TrES-5. Green, red and black points show the *g*, *r*, and *i* data, respectively.

Table 4. Spectroscopic properties of the host stars in the Qatar-1 and TrES-5 systems adopted from the literature.

Source	Qatar-1	Ref.	TrES-5	Ref.
$T_{\rm eff}$ (K)	4910 ± 100	1	5171 ± 36	2
$\left[\frac{\rm Fe}{\rm H}\right]$ (dex)	0.20 ± 0.10	1	0.20 ± 0.10	2
$K_{\rm A}$ (m s^{-1})	265.7 ± 3.5	1	339.8 ± 10.4	2

References: (1) Covino et al. (2013), (2) Mandushev et al. (2011).

indicators of the presence of star-spots. This is at least partly due to the relative faintness of TrES-5 ($V = 13.7$), at least for a 2-m class telescope equipped with an instrument containing many optical elements.

4 PHYSICAL PROPERTIES

We determined the physical properties of the two systems from the light-curve fits (the weighted means in Tables 2 and 3), from the spectroscopic measurements of host star's atmospheric properties, and from the tabulated predictions of five different sets of theoretical stellar evolutionary models. The values of $r_{\rm A}$, $r_{\rm b}$, and i in Tables 2 and 3 were combined according to their weighted mean, inflating the resulting error bars to enforce $\chi^2_\nu = 1.0$ for each quantity. The spectroscopic measurements of the stellar effective temperature ($T_{\rm eff}$), metallicity ($\left[\frac{\rm Fe}{\rm H}\right]$), and orbital velocity amplitude ($K_{\rm A}$) were taken from published studies and are summarized in Table 4. Tabulated predictions were obtained from the Claret (2004a), Y^2 (Demarque et al. 2004), Teramo (Pietrinferni et al. 2004), VRSS (VandenBerg, Bergbusch & Dowler 2006), and DSEP (Dotter et al. 2008) stellar models.

For each target we began by estimating a value for the velocity amplitude of the *planet*, $K_{\rm b}$, allowing us to calculate a set of physical properties for the system using standard formulae. The value of $K_{\rm b}$ was then iteratively refined to maximize the agreement between the observed and predicted $T_{\rm eff}$, and the measured $r_{\rm A}$ and predicted $\frac{R_{\rm A}}{a}$. Finally, the full procedure was undertaken using each of the five sets of stellar model predictions. For both objects we assumed a circular orbit, based on the conclusions of Covino et al. (2013) and Mandushev et al. (2011). We used the set of physical constants given by Southworth (2011).

The uncertainties on the input parameters were propagated through the analysis using a perturbation approach, and added in quadrature to give the final random error. A systematic error bar was also estimated based on the interagreement between the results obtained using each of the five different model sets. Table 5 gives our final physical properties, random error bars for all quantities, and systematic error bars for those results which depend on stellar theory.

Also, only for Qatar-1A, we were able to calculate the stellar rotation period. Thus, we can use gyrochronology model to estimate stellar the age of Qatar-1b host star. Using the model from Barnes (2007) and stellar rotation period 23.697 d and $B - V = 1.06$, we estimate the age of Qatar-1A $\tau_g = 1.1865 \pm 0.47$ Gyr.

Our final results for Qatar-1 are in good agreement with published studies (Alsubai et al. 2011; Covino et al. 2013), and yield a significant improvement in precision. In the case of TrES-5 we agree with the findings of Mandushev et al. (2011) but do not obtain significantly smaller error bars. This is because we account for systematic errors whereas Mandushev et al. (2011) do not, and also because the errors estimated by Mandushev et al. (2011) appear to be too small (for example they claim that the orbital inclination is $i = 84.^\circ529 \pm 0.^\circ005$, a level of precision not normally achieved even with *Kepler* or *Hubble Space Telescope* light curves). Our results are therefore to be preferred to those of Mandushev et al. (2011) because they are based on a larger and more precise data set, and because our error bars have been more robustly calculated.

5 RESULTS AND CONCLUSIONS

We present extensive optical photometry of transit events in two extrasolar planetary systems with K-dwarf host stars. Our data comprise 12 light curves of Qatar-1 and eight light curves of TrES-5. These data include simultaneous observations in three passbands of one transit for each object. We use these data to search for star-spot crossing events during transit, with a negative result. We do, however, measure the rotational period of $P_\star = 23.697 \pm 0.123$ d for Qatar-1A from the survey photometry in its discovery paper, showing that this does display spot activity. The corresponding rotational velocity is close to the $v \sin i_\star$ value measured from an observation of the Rossiter–McLaughlin effect in this system, so its low projected orbital obliquity also implies a low true orbital obliquity. The

Table 5. Derived physical properties of the two systems. Where two sets of error bars are given, the first is the statistical uncertainty and the second is the systematic uncertainty.

Quantity	Symbol	Unit	Qatar-1	TrES-5
Stellar mass	$M_{\rm A}$	$M_\odot$	$0.818 \pm 0.047 \pm 0.050$	$0.901 \pm 0.029 \pm 0.008$
Stellar radius	$R_{\rm A}$	$R_\odot$	$0.796 \pm 0.016 \pm 0.017$	$0.868 \pm 0.013 \pm 0.002$
Stellar surface gravity	$\log g_{\rm A}$	c.g.s.	$4.549 \pm 0.011 \pm 0.009$	$4.517 \pm 0.012 \pm 0.001$
Stellar density	$\rho_{\rm A}$	$\rho_\odot$	1.621 ± 0.046	1.381 ± 0.051
Planet mass	$M_{\rm b}$	$M_{\rm Jup}$	$1.293 \pm 0.052 \pm 0.054$	$1.790 \pm 0.067 \pm 0.010$
Planet radius	$R_{\rm b}$	$R_{\rm Jup}$	$1.142 \pm 0.026 \pm 0.024$	$1.194 \pm 0.015 \pm 0.003$
Planet surface gravity	$g_{\rm b}$	m s^{-2}	24.56 ± 0.70	31.1 ± 1.0
Planet density	$\rho_{\rm b}$	$\rho_{\rm Jup}$	$0.811 \pm 0.036 \pm 0.017$	$0.983 \pm 0.039 \pm 0.003$
Equilibrium temperature	$T'_{\rm eq}$	K	1388 ± 29	1480 ± 13
Safronov number	Θ		$0.0640 \pm 0.0017 \pm 0.0014$	$0.0817 \pm 0.0028 \pm 0.002$
Orbital semi-major axis	a	au	$0.023\,13 \pm 0.000\,44 \pm 0.000\,48$	$0.024\,59 \pm 0.000\,26 \pm 0.0007$
Age (gyrochronology)	$\tau_{\rm g}$	Gyr	1.19 ± 0.47	

lack of observed spot crossings may be due to the planets crossing latitudes of the stars which show low spot activity, i.e. the planetary chords miss the active latitudes of the stellar surfaces.

We use our data to measure the photometric parameters of both systems. When combined with published spectroscopic quantities, these yield precise measurements of the full physical properties of the systems. Qatar-1 and TrES-5 have notable similarities in their respective stellar properties, and planetary equilibrium temperature, radius and density. Our results also yield refined measurements of the orbital ephemerides of the systems.

ACKNOWLEDGEMENTS

This publication is supported by NPRP grant no. X-019-1-006 from the Qatar National Research Fund (a member of Qatar Foundation). The statements made herein are solely the responsibility of the authors.

Based on observations obtained with the 1.52-m Cassini telescope at the OAB Observatory in Loiano (Italy), and with the 1.23-m and 2.2-m telescopes at the Centro Astronòmico Hispano Alemàn (CAHA) at Calar Alto (Spain), jointly operated by the Max-Planck Institut for Astronomy and the Instituto de Astrofìsica de Andalucìa (CSIC).

We thank to TÜBİTAK for the partial support in using T100 telescope with project number 12CT100-378. OB acknowledges the support by the research fund of Ankara University (BAP) through the project 13B4240006.

REFERENCES

Alonso R. et al., 2004, ApJ, 613, L153
Alonso R., Barbieri M., Rabus M., Deeg H. J., Belmonte J. A., Almenara J. M., 2008, A&A, 487, L5
Alsubai K. A. et al., 2011, MNRAS, 417, 709
Alsubai K. A. et al., 2013, Acta Astron., 63, 465
Barnes S., 2007, ApJ, 669, 1167
Claret A., 2004a, A&A, 424, 919
Claret A., 2004b, A&A, 428, 1001
Covino E. et al., 2013, A&A, 554, A28
Demarque P., Woo J.-H., Kim Y.-C., Yi S. K., 2004, ApJS, 155, 667
Dotter A., Chaboyer B., Jevremović D., Kostov V., Baron E., Ferguson J. W., 2008, ApJS, 178, 89
Mancini L. et al., 2014, MNRAS, 443, 2391
Mandushev G. et al., 2011, ApJ, 741, 114
Mislis D., Schröter S., Schmitt J. H. M. M., Cordes O., Reif K., 2010, A&A, 510, A107
Nutzman P. A., Fabrycky D. C., Fortney J. J., 2011, ApJ, 740, L10
Oshagh M., Santos N. C., Ehrenreich D., Haghighipour N., Figueira P., Santerne A., Montalto M., 2014, A&A, 568, A99
Pietrinferni A., Cassisi S., Salaris M., Castelli F., 2004, ApJ, 612, 168
Pont F., Sing D. K., Gibson N. P., Aigrain S., Henry G., Husnoo N., 2013, MNRAS, 432, 2917
Sanchis-Ojeda R., Winn J. N., Holman M. J., Carter Joshua A., Osip D. J., Fuentes C. I., 2011, ApJ, 733, 127
Southworth J., 2008, MNRAS, 386, 1644
Southworth J., 2009, MNRAS, 394, 272
Southworth J., 2011, MNRAS, 417, 2166
Southworth J. et al., 2009, MNRAS, 396, 1023
Southworth J. et al., 2014, MNRAS, 444, 776
Tregloan-Reed J., Southworth J., Tappert C., 2013, MNRAS, 428, 3671
VandenBerg D. A., Bergbusch P., Dowler P., 2006, ApJS, 162, 375
von Essen C., Schröter S., Agol E., Schmitt J. H. M. M., 2013, A&A, 555, A92

This paper has been typeset from a TEX/LATEX file prepared by the author.